



Spectral Indices Based Study to Evaluate and Model Surface Water Quality

of Beni Suef Governorate, Egypt

Mahmoud Saad¹, Salwa Elbeih², Essam Abdel Rahman³, Hend S. abu Salem⁴,

Mohammed Ibrahim⁵, El-Sayed El-Bastamy⁶



¹Beni-Suef University, Faculty of Science, Geology Department

²National Authority for Remote Sensing and Space Sciences, Cairo, Egypt

³Beni-Suef University, Faculty of Earth Science, Geology Department

⁴Cairo University, Faculty of Science, Geology Department

⁵Beni-Suef University, Faculty of Science, Geology Department

⁶Central Laboratory for Environmental Quality Monitoring (CLEQM), NWRC, Egypt.

Abstract

Beni Suef governorate is one of highly population density areas in northern Upper Egypt. The surface water in Beni Suef district suffer from pollution due to the impact of anthropogenic activities such as usage of fertilizers and pesticide, waste disposal, industrial wastes and wastewater. The present study aims to estimate the Water Quality Index (WQI) and concentration of some other parameters through applying water quality estimation models based on Remote Sensing techniques applied on Landsat 8 OLI satellite images. Thirty-four points distributed among the study area are used for the analysis and to compare the data with the results obtained from analyzing water samples tested in the laboratory to investigate the feasibility of utilizing remote sensing data to identify water quality. In the present study, integrated technologies of remote sensing and water quality have been successfully utilized to assess water pollution in the study area and give an explanation for the influence of urbanization, cultivation and other human activities on water quality. The results showed that there are four classes of WQI for surface water samples, about 6 % belong to the excellent class, 65% to good class, 20.6% to poor class and the rest of samples belong to very poor class, while no samples belong to unsuitable class. It could be noted that the very poor category of WQI belongs to Bahr Yusef Canal. on other hand the main classes obtained from the supervised classification show that the agricultural land dominated the whole study area with 75%, which might have an impact on water quality in the study area. The second dominant class is represented by urban areas with 11%. The third class was bare land with 10 %, which are distributed in several separate parts in the study area. The fourth class represented by water bodies with 4%. The most appropriate models which calculated from water indices, band ratios and combination bands of the satellite image for the study area are very significant to detect water quality parameters. They also show the same results as the set of field data which measured from the laboratory tests. It is recommended to continue in the study of water quality by remote sensing techniques.

Keywords: Water quality, Remote sensing, , Water pollution, Surface water, Beni Suef Governorate.

1. Introduction

Water is described as a life-giving, sustaining, and purifying natural resource and it is the origin of all life on Earth. With advance and increasing role of technology, new techniques and methods are developed for assessing water quality such as Remote Sensing and Geographical Information Systems (GIS).

Remote sensing refers to techniques used in collection and interpretation of information about the Earth's surface without being in contact with it [1].

Each type of earth surface features; water bodies, vegetation, soils and rocks, reflects or emits an electromagnetic radiation in a characteristic style. The most common component in remote sensing is the satellite which carries a sensor that receives electromagnetic radiation and converts it into a signal that can be recorded and displayed as either numerical data or an image [2]. There are several previous studies which have used remote sensing and GIS techniques for the water quality parameters. The study of Carlson

*Corresponding author e-mail: Mahmoudsad2000@Gmail.com.

Receive Date: 24 December 2021, Revise Date: 07 February 2022, Accept Date: 20 February 2022

DOI: 10.21608/EJCHEM.2022.112759.5121

©2022 National Information and Documentation Center (NIDOC)

and Ecker, [3], focused on the comparison of the types of water in two lakes; Silver and Casey in USA, whether each lake was changed or not in terms of the water quality variables of the year (1999 to 2000). The study of Dewidar and Khedr [4], showed the use of Landsat Thematic Mapper (TM) data combined with surface measurements for mapping water quality parameters of Burullus Lake. Fadel [5] applied Normalized Difference Vegetation Index (NDVI), Normalized Difference Water Index (NDWI) and Tasseled Cap indices on multi-time Landsat images. This study shows the efficiency of remote sensing techniques and geographic information systems in discovering and assessing the environmental changes. Ming et al., [6] have established integrated water quality models with GIS techniques in central Taiwan. The model is based on the band ratio regression to show the water quality conditions for remote sensing monitoring. The study of Yas [7], used remote sensing with GIS techniques for studying the hydro chemical properties of the water of the Himreen Dam reservoir on Diyala river. The spectral reflectance of the Landsat image was correlated with some quality parameters which were analyzed at the same period of Landsat image. The results showed that there was a high correlation between spectral reflectance of the image with turbidity and reservoir depth. The study of Abdelmalik [8] showed the presence of relationship between ASTER data and the observed water quality parameters for Qaroun Lake in Fayoum, Egypt. Relationship between spectral data and water quality has been widely utilized in spatiotemporal and regional assessment of water pollution [9].

The aim of this study is to measure some water quality parameters in order to determine the Water Quality Index (WQI) and using mathematical relationship such as regression models between water quality parameters as independent variables and spectral bands of Landsat 8 OLI as dependent variables and compare the results with the observed field data.

2. Study Area

Beni Suef governorate is located in the Nile Valley and occupies an area of about 10,950 km², bounded by the eastern and western deserts. About 75% of the total populated area is agricultural land. Surface water, mostly represented by River Nile, Al Ibrahimia Canal, Bahr Yusef and Al Gizawia Canal is considered the major source to ensure water demand for different purposes. The study area is located along the western bank of the Nile valley, occupies alluvial plains, and is located between latitudes 28° 45' 00" , 29° 24' 00" N and longitudes 30° 47' 20" , 31° 14' 13" E. It extends from the River Nile in the east to Bahr Yusef Canal in

the west and from El-Fashn city at the south to Al Wasta city at the north, (Fig. 1).

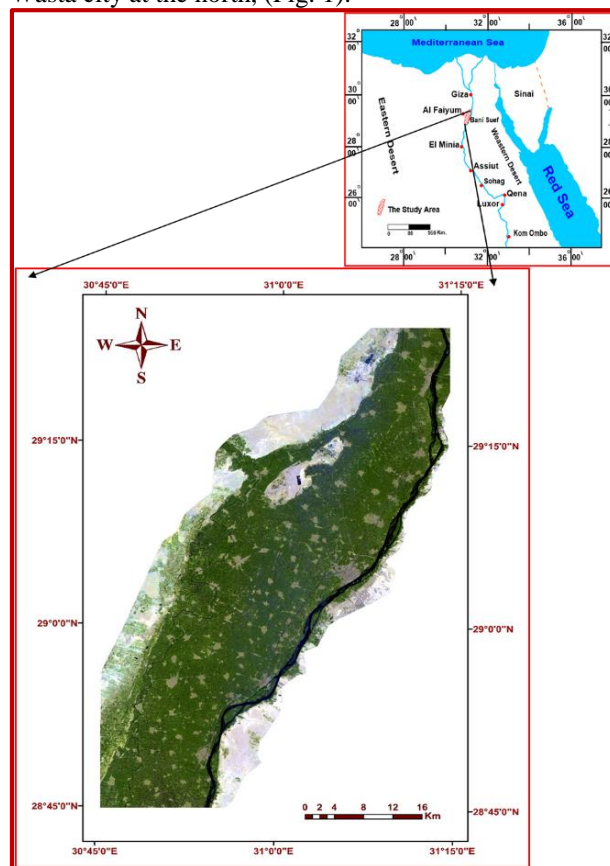


Fig. (1) Location map of the study area in Beni Suef governorate.

3. Materials and Methods

In order to achieve the objectives of the present study, data was collected through several field trips as follows:

1. Collection and analysis of surface water samples from the study area to perform a group of physiochemical and bacteriological tests [10] in the Central Laboratory for Environmental Quality Monitoring in Cairo (National Water Research Center), taking into account the parameters measured in the field (i.e temperature, pH, electrical conductivity, dissolved oxygen) using some portable devices, GPS (Global Position System) to detect the geographic location of the selected station points (Table 1).
2. Collection and analysis of periodical records for the climatic data during the last twenty years, from the Egyptian Meteorological Authority.
3. Using topographic maps, shape files, of Beni Suef Governorate to prepare the base map and the monitoring points map of the study area.

4. Preparing all the graphical representations and maps for analytical results using some computer programs as Surfer Ver. (19), Grapher Ver. (15), geographic information system (QGIS), Groundwater for windows (modified object vision, Reference Guide, by Borland 1991 (GWW), Diagrammes, Geochemist's Workbench Community Edition 15.0, SPSS, Ver. (23) and Microsoft office Ver. (365) programs.
5. The remotely sensed image data used in this study includes Landsat-8 (OLI) images. The images are downloaded from the United States Geological Survey (USGS), Earth Explorer (EE) website. The images date is 17/August/ 2018). Atmospheric and radiometric correction were applied to the image using ENVI software, Also, the digital number (DN) is converted to reflections and the result is clearly represented by surface reflection as will mentioned later. The conversion process take place by using QGIS software.
6. Evaluating the surface water quality through some spectral indices obtained from satellite RS images.

3.1. Water Quality Index (WQI)

The water quality index (WQI) is a mathematical tool used to transform some Parameters of water characterization data into a single number that represents the water quality level [11].

For calculation of WQI, a particular weightage (W_a) was given to each water quality parameter according to its relative importance on the overall quality of water which ranges from 1 to 5. Parameters which have more importance on the water quality were give weight 5 while the least importance one was given a weight of 1 [12]. To calculate WQI, thirteen parameters of water were selected. These were pH, total dissolved solids (TDS), total hardness (TH), total alkalinity (TA), chloride (Cl), sulphate (SO₄), manganese (Mn), magnesium (Mg), calcium (Ca), Sodium (Na), Copper (Cu), iron (Fe) and zinc (Zn). The relative weights (W_r) of all factors were calculated (Table 2) based on the equation:

$$W_r = \frac{w_{ai}}{\sum_{i=1}^n w_{ai}} \quad \text{Eq. 1}$$

where W_r = relative weight,

Table (1): The location of the sample stations in the study area, Beni Suef governorate.

Sample No.	Longitude (E)	Latitude (N)	Water source
1	31.1076	29.0948	Al Ibrahimia Canal
2	31.0731	29.0393	Nile River
3	31.0998	29.0602	Nile River
4	30.9813	28.9241	Al Ibrahimia Canal
5	31.0073	28.9914	Al Ibrahimia Canal
6	30.9564	28.8934	Nile River
7	31.0033	28.9319	Nile River
8	30.9897	28.9241	Nile River

W_a =assigned weight of each parameter,

n = number of parameters

Then, quality rating scale (Q_i) has been measured for each parameter using Eq. 2. The standard values of each parameter were specified according to the WHO guidelines [13]. The ideal value (V_i) of pH is equal to 7, whereas for all other parameters, $V_i = 0$. (Table 3), shows the WQI classification on a scale suggested by [14].

Table (3). Water Quality Index scale.

Water quality	WQI
Excellent	0-25
Good	26-50
poor	51-75
Very poor	76-100
Unsuitable	>100

$$Q_i = ([C_i - v_i]/[S_n - V_i]) * 100 \quad \text{Eq. 2}$$

where Q_i = quality rating scale,

C_i = measured concentration of each parameter,

S_n = drinking water standard values for each parameter.

Then, the sub-indices (SI) have been calculated using the next equations:

$$SI_i = Q_i * W_r \quad \text{Eq. 3}$$

Finally,

$$WQI = \sum_{i=1}^n SI_i \quad \text{Eq. 4}$$

3.2. Remote Sensing Data Pre-processing

Before data analysis, initial processing on the raw data is carried out to correct for any distortion due to the characteristics of the imaging system and imaging conditions. Radiometric corrections may be necessary due to variations in scene illumination and viewing geometry, atmospheric conditions, and sensor noise and response. While geometric correction used for correct geometric errors in the data acquisition system and to register the satellite image to a map projection, [15].

In this study it is appropriate to include some procedures to convert the raw, unitless relative reflectance values, known as digital numbers, or DN, of the original bands into true measures of reflective power (radiance), according to the following equations, [16]:

9	30.9293	28.8831	Nile River
10	31.0169	28.9521	Nile River
11	30.7973	28.7563	Bahr Yusef canal
12	30.7992	28.7946	Bahr Yusef canal
13	30.9007	28.8218	Al Ibrahimia Canal
14	30.9118	28.775	Nile River
15	30.9115	28.7873	Nile River
16	30.8003	28.8879	Bahr Yusef canal
17	30.8005	28.865	Bahr Yusef canal
18	30.8667	28.9849	Bahr Yusef canal
19	30.9495	29.178	Bahr Yusef canal
20	30.9119	29.0511	Bahr Yusef canal
21	31.1585	29.1831	Al Ibrahimia Canal
22	31.2016	29.2086	Nile River
23	31.2076	29.2184	Nile River
24	31.149	29.1215	Nile River
25	31.1896	29.1904	Nile River
26	31.1057	29.2907	Al Gizawia Canal
27	31.1274	29.322	Al Gizawia Canal
28	31.0775	29.2712	Al Gizawia Canal
29	31.1647	29.3751	Al Gizawia Canal
30	31.209	29.3398	Nile River
31	31.2076	29.2436	Nile River
32	31.222	29.3675	Nile River
33	31.229	29.3874	Nile River
34	31.1666	29.3968	Al Gizawia Canal

Table (2). Computation methodology of Water Quality Index.

Parameters	W_a	W_r	S_n	V_i
pH	3	0.069767442	8.5	7
TDS	5	0.11627907	1000	0
TH	2	0.046511628	500	0
TA	2	0.046511628	500	0
Cl	3	0.069767442	250	0
SO ₄	3	0.069767442	250	0
Ca	2	0.046511628	200	0
Mg	2	0.046511628	100	0
Na	3	0.069767442	200	0
Cu	4	0.093023256	1	0
Fe	5	0.11627907	0.3	0
Mn	5	0.11627907	0.1	0
Zn	4	0.093023256	3	0

$\rho\lambda' = M^P \times Qcal + A^P$ Eq. (5)
 $\rho\lambda'$ top-planetary spectral reflectance, without correction for solar angle

M^P reflectance multiplicative rescaling factor from the metadata for band (REFLECTANCE _ MULT_BAND_ x, where x is the band number) = 2.0000e-05

$Qcal$ reflectance additive rescaling factor from the metadata for the Band (REFLECTANCE _ ADD_BAND_ x, where x is the band number) = -0.1
 A^P quantized and calibrated standard product pixel values (DN)

Correction for the solar elevation angle represented an important factor to calculate top of atmosphere (TOA) reflectance with a correction for the sun angle as in the following equation below:

$$P\lambda = \rho\lambda' / \sin(\theta) \quad \text{Eq. (6)}$$

Where:

$P\lambda$ top-of-atmosphere planetary reflectance

(θ) solar elevation angle (from the MTL file of the OLI raw data) = 63.2466°

3.3. Statistical analysis (Correlation and Regression)

This analysis aims to find the statistical relation between water quality parameters during the field Survey and the values extracted from spectral band of satellite image (Landsat-8). To assess the nature and strength of the relationships, Pearson correlation (r) using correlation coefficient and simple linear regression are using, then the highly correlated value represents the best index.

- Correlation

There are three different types of correlation coefficients which are in use. The Karl-Pearson correlation coefficient is more usually used in measuring the relationship between two variables, and it has been considered in this study, as shown in the following equation, [17]:

$$r = \frac{n(\sum xy) - (\sum x)(\sum y)}{\sqrt{[n(\sum x^2) - (\sum x)^2][n(\sum y^2) - (\sum y)^2]}} \quad \text{Eq.7}$$

Where:

r value of the correlation coefficient
 n number of observations
 $\sum x$ the summation variable x (x1, x2, x3,.....).
 $\sum y$ the summation variable y (y1, y2, y3,.....).

The coefficient of determination (R^2) is used to explain how much variability of one factor can be caused by its relationship to another factor.

The formula for computing the coefficient of determination for a linear regression model, as shown in the following, [18]:

$$R^2 = r^2 \quad \text{Eq.8}$$

Where:

r^2 Square correlation coefficient.

- Linear regression models

It is one of the most widely used statistical tools because it provides simple methods for establishing a functional relationship among variables.

- Simple Regression: used for studying the relationship between a pair of variables that show in a data set, as shown in the following equation:

$$Y = \beta_0 + \beta_1 x \quad \text{Eq.9}$$

Where: β_0 and β_1 are regression coefficients
 X independent variable in the model.
 Y dependent variable.

- Multiple Regressions: used for studying the relationship between one (dependent) variable and several of other (independent) variables, as shown in the following equation:

$$Y = \beta_0 + \beta_1 x_1 + \beta_2 x_2 + \dots + \beta_n x_n \quad \text{Eq.10}$$

Where:

$\beta_0, \beta_1, \beta_2, \dots, \beta_n$ regression coefficients.
 X_1, X_2, \dots, X_n independent variables in

the model.

Y dependent variable.

4. Results and Discussion

The calculated WQI values for each water sample (Fig. 2), illustrates that there are four classes of WQI for surface water samples, about 6 % belong to the excellent class, 65% to good class, 20.6% to poor class and the rest of samples belong to very poor class, while no samples belong to unsuitable class. It could be noted that the very poor category of WQI belongs to Bahr Yusef Canal as shown in Fig. (3).

4.1. Digital data processing

Earth's surface features have different reflection properties in different wavelength bands, so the processing of the bands in different combinations allows them to be identified and separated. Reflectance for two features may be very similar in one part of the spectrum and very different in another part.

The reflectance in water surface depends up on the suspended sediments, the chemical contents disbanded in the water or plants and animals at the bottom of the water. The surface reflectance of Landsat-8(OLI) bands for selected stations according to the Equations [(5) and (6)] as mentioned before, are shown in Figure (4) and Table (4), where the station points with higher values of reflectance belong to Al Ibrahimia canal, Baher Yusef canal and AlGizawia canal because they have width range from 15m to 20m which is equivalent to less than one pixel, so the pixel is a mixture of water, vegetation and soil, this is the reason of increasing in reflectivity with a set of points. On other hand, the Nile River has width more than 30m i.e., equivalent to more than one pixel, that is caused decreasing in reflectivity in the station points belong to Nile River.

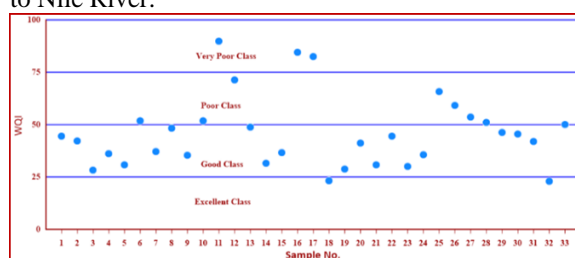


Fig. (2): WQI for the surface water samples in the study area.

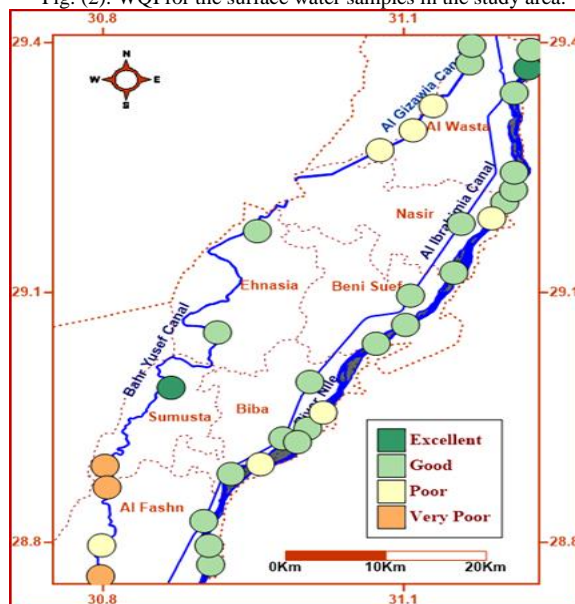


Fig. (3): Distribution of WQI classes for the surface water samples in the study area.

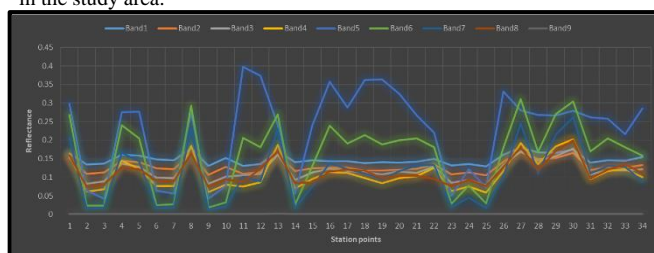


Fig. (4): Surface reflectance for Landsat 8(OLI) bands for selected stations in the study area.

4.2. Image classification

Landsat 8 data support a wide collection of applications such as, mapping coastal water areas, differentiation between soil and vegetation, forest type mapping, geological boundary delineation, crop identification, and land-water contrasts. Therefore, the Landsat 8 data have been used in the present study to determine the water quality of surface water.

Image classification is a technique applied to derive different landcover types from remote sensing images. There are two general types of image classification, supervised and unsupervised classification. In unsupervised classification, the computer software automatically groups the pixels in the image into separate classes, depending on their spectral features. Each class represents a land cover type. In the case of supervised classification, the computer software detects individual landcover types based on statistical characterization data getting from a known examples in the image, known as, training sites.

In this study, supervised classification has been applied on the images using Maximum Likelihood Method. The training samples, region of interests, have been selected based on land cover and terrain. Four different land cover classes were selected including water, vegetation, urban areas and bare lands.

Figure (5) show the results of supervised classification. From the main classes obtained, the agricultural land dominated the whole study area with 75%, which might have an impact on water quality in the study area. The second dominant class in the study area is represented by urban areas with 11%. The third class was bare land with 10 %, which are distributed in several separate parts in the study area. The fourth class represented by water bodies with 4%. The accuracy of the supervised classification was supported by the indices maps, NDBI, NDVI and NDWI, Figs. (6 ,7 and 8).

Table (4): Surface reflectance for the nine bands for the selected stations in the study area.

Sample	Band1	Band2	Band3	Band4	Band5	Band6	Band7	Band8	Band9
1	0.1650708	0.1525729	0.156313	0.162517	0.298091	0.267585	0.206574	0.159001	0.001344
2	0.1342516	0.1089871	0.082468	0.061862	0.063385	0.023361	0.014379	0.073576	0.001277
3	0.136357	0.1127947	0.088695	0.067215	0.042981	0.024122	0.018456	0.07996	0.001299
4	0.1604345	0.1440618	0.136671	0.144375	0.275066	0.239924	0.165519	0.12704	0.001053
5	0.1585979	0.1404782	0.128473	0.123613	0.277194	0.204558	0.143121	0.121418	0.000896
6	0.148071	0.1241055	0.098998	0.076152	0.064214	0.025332	0.015947	0.090016	0.001456
7	0.145876	0.1218433	0.097945	0.076779	0.056487	0.027818	0.018769	0.089568	0.001187
8	0.1783303	0.1646453	0.164175	0.184669	0.272333	0.292738	0.231749	0.164153	0.000985
9	0.1305784	0.1067473	0.082983	0.060138	0.042556	0.018657	0.012386	0.074293	0.001075
10	0.1515426	0.1276219	0.101999	0.079601	0.076533	0.032432	0.020449	0.093622	0.001209
11	0.1308472	0.1091215	0.105515	0.075122	0.397715	0.205611	0.102245	0.08818	0.001187
12	0.1350356	0.1147433	0.108741	0.086029	0.373593	0.181444	0.089501	0.123232	0.000874
13	0.1703119	0.1612184	0.161398	0.186886	0.241402	0.269354	0.229487	0.170334	0.001657
14	0.140299	0.1167143	0.09295	0.06997	0.056599	0.025892	0.016664	0.083745	0.001209
15	0.1453385	0.1242623	0.112414	0.094921	0.240305	0.129996	0.075749	0.086388	0.001053
16	0.1428747	0.1254046	0.123254	0.113982	0.356795	0.239207	0.137544	0.114967	0.001478
17	0.1433451	0.1253374	0.116781	0.112033	0.28828	0.191478	0.121933	0.120679	0.001344
18	0.1377905	0.1180581	0.112929	0.098438	0.362439	0.213987	0.11051	0.11761	0.001165
19	0.140187	0.1183269	0.107576	0.083454	0.363514	0.188723	0.094989	0.098393	0.00103
20	0.1398063	0.1200291	0.115706	0.09846	0.324856	0.199832	0.117252	0.10444	0.000874
21	0.1415981	0.1224705	0.111406	0.10294	0.267003	0.204849	0.132079	0.104687	0.001321
22	0.1491685	0.1344756	0.128742	0.125046	0.219878	0.180548	0.133692	0.095011	0.000784
23	0.1313175	0.107912	0.084641	0.062198	0.050507	0.02896	0.020382	0.07707	0.001053
24	0.135058	0.1125931	0.092928	0.074831	0.121418	0.077653	0.045131	0.092435	0.000918
25	0.1294361	0.1057394	0.079221	0.058256	0.072658	0.029968	0.016955	0.076667	0.000985
26	0.1607481	0.1417997	0.133266	0.116356	0.330903	0.179271	0.102716	0.12798	0.001277
27	0.1796293	0.1678257	0.169147	0.192575	0.280732	0.310499	0.245658	0.18122	0.001344
28	0.1676018	0.1500644	0.144667	0.135551	0.26819	0.168005	0.110689	0.119604	0.001165
29	0.1662579	0.1521922	0.1575	0.184064	0.266264	0.270116	0.215488	0.171454	0.001254
30	0.174993	0.1664595	0.176785	0.202878	0.278694	0.304698	0.261403	0.199944	0.000896
31	0.138776	0.1195812	0.107845	0.095795	0.262053	0.170066	0.109883	0.09678	0.001344
32	0.1454953	0.128585	0.119604	0.117073	0.258312	0.204715	0.130825	0.120746	0.000874
33	0.1446442	0.1260541	0.117409	0.121283	0.216294	0.181556	0.128428	0.133736	0.000806
34	0.1541856	0.132975	0.121194	0.100924	0.28566	0.158083	0.088448	0.111764	0.001097

Fig. (5): Land cover in the study area.

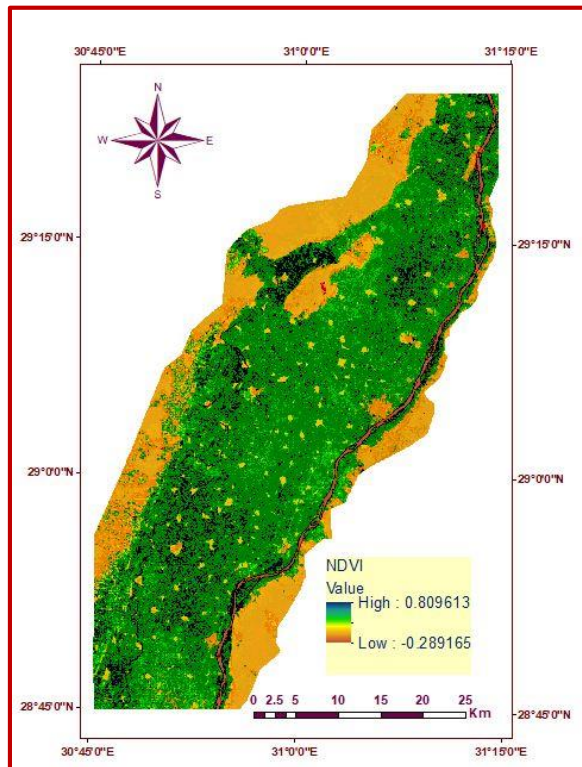
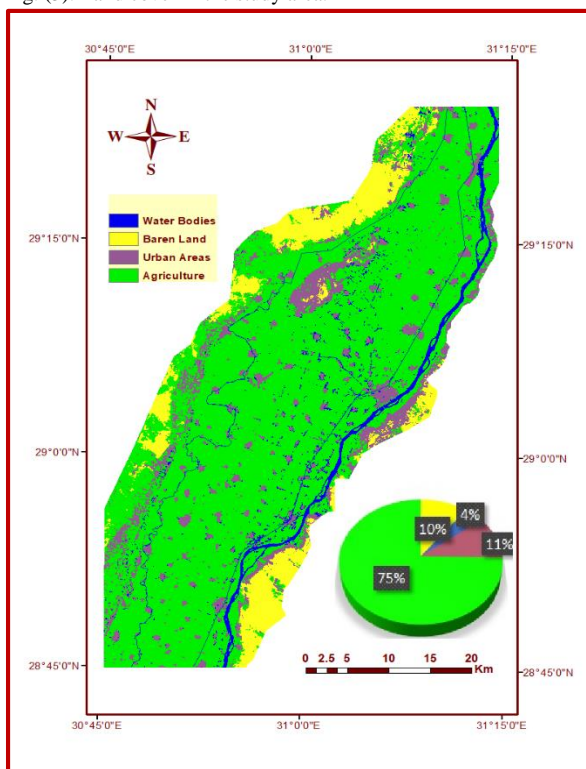


Fig. (7): NDVI in the study area.

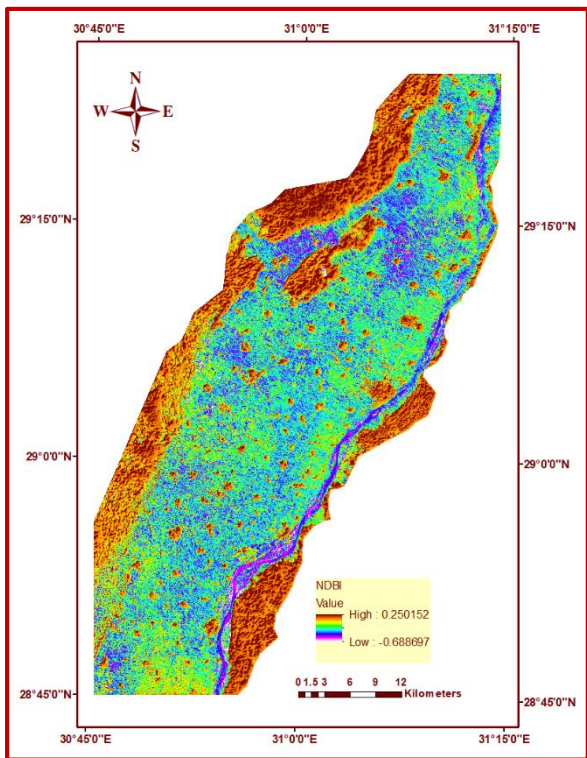


Fig. (6): NDBI in the study area.

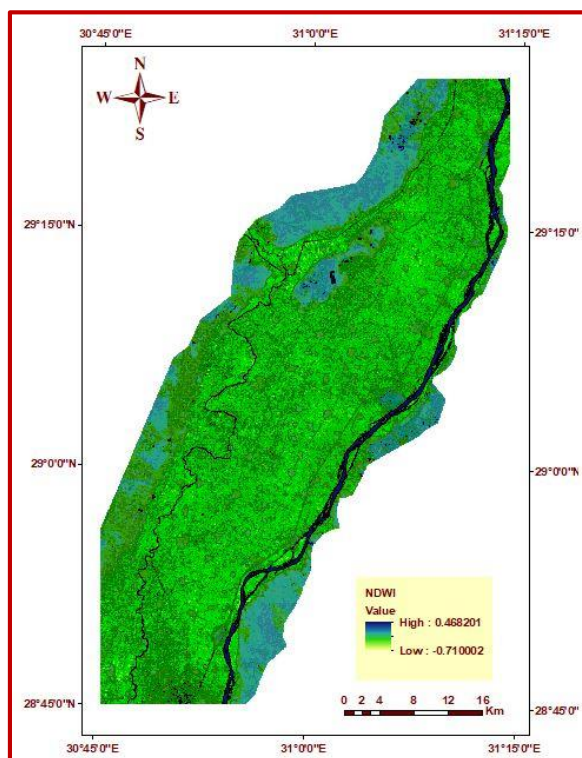


Fig. (8): NDWI in the study area.

4.3. Image Transforms

Although they are not strictly transforming, where these operations permit the creation of a derived image which may be separate spectral bands from a single multispectral data set, or they may be individual bands from image data sets that have been collected on different dates. The derived image may well have properties that make it more suitable for a particular purpose than the original [19].

The term "transform" used for the arithmetic procedures of subtraction, addition, division, and multiplication.

- **Band combination:**

It is used for enhancing the spectral differences between bands and to reduce the effects. Combination of one spectral band with another produces an image that provides relative band intensities.

The band combinations used in this study are included, (B+C), (B+G), (B+R), (B+NIR), (B+G+C), (B+G+R), (B+G+NIR), (B+R+NIR), (B+R+C), (C+B+G+R), (C+B+G+NIR), (B+C+NIR), (G+C), (G+R), (R+NIR), (C+NIR), (G+C+R), (G+R+NIR) and (R+C+NIR), Table (5).

- **Band ratios:**

It represents one of the spectral enhancement techniques which represent the ratio between digital numbers for two or more different bands.

Ratio and combination bands can often provide information that cannot be obtained from the band singly.

The band ratios used in this study are included, (B/C), (B/G), (B/R), (B/NIR), (C/B), (C/G), (C/R), (C/NIR), (G/C), (G/B), (G/R), (G/NIR), (R/C), (R/G), (R/B), (R/NIR), (NIR/B), (NIR/G), (NIR/R), (B/(R+C)), (B/(R+B)), (B/(NIR+C)), (NIR/(B+G)), (NIR/(B+R)) and (NIR/(B+NIR)), Table(6).

- **Spectral index:**

It is a mathematical equation that is applied on different spectral bands used for detection the relative abundance of features of interest. It is very effective for interpretation and analysis of phenomena and processes related to the dynamics of change of the main components of the Earth surface. There are several different equations that can be applied on the spectral to produce a spectral index. Table (7) show the indices used in the study area.

The indices using in this study are included:

Table (5): Band combinations used in the study area.

Sample	(C+B+G+R)	(C+B+G+NIR)	(B+R+C)	(B+C+NIR)	(C+NIR)	(G+C+R)	(G+R+NIR)
1	0.6365	0.7720	0.4802	0.6157	0.4632	0.4839	0.6169
2	0.3876	0.3891	0.3051	0.3066	0.1976	0.2786	0.2077
3	0.4051	0.3808	0.3164	0.2921	0.1793	0.2923	0.1989
4	0.5855	0.7162	0.4489	0.5796	0.4355	0.4415	0.5561
5	0.5512	0.7047	0.4227	0.5763	0.4358	0.4107	0.5293
6	0.4473	0.4354	0.3483	0.3364	0.2123	0.3232	0.2394
7	0.4424	0.4222	0.3445	0.3242	0.2024	0.3206	0.2312

- Normalized difference water index (NDWI), [20]
NDWI= (GREEN-NIR) / (GREEN+NIR)
- Modification of normalized difference water Index (MNDWI), [21]
MNDWI= (GREEN-SWIR2) / (GREEN+ SWIR2)
- Normalized difference moisture index (NDMI), [22]
NDMI=(RED-NIR) / (RED +NIR)
- Automated water extraction index (AWEI), [23]
AWEI= 4*(GREEN-SWIR2) - (0.25*NIR+2.75*SWIR1)
- Water ratio index (WRI), [24]
WRI= (GREEN+ RED) / (NIR + SWIR2)
- Ratio vegetation index (RVI), [25]
RVI = NIR / RED
- Infrared personage vegetation index (IPVI), [26]
IPVI= NIR / (NIR+ RED)
- Different vegetation index (DVI), [27]
DVI=NIR-RED
- Normalized difference vegetation index (NDVI), [28]
NDVI= (NIR- RED) / (NIR+ RED)

4.4. Water quality parameters from field measurement and satellite images

Water quality parameters from Landsat -8 OLI spectral bands had been estimated in this study using statistical methods and by using SPSS software. The values of regression equations for each water quality parameter are calculated according to Eq. (7,8 and 10) mentioned before. Selection of the model parameters was based on the Pearson correlation between water quality parameters and the spectral reflectance characteristics. Where the most appropriate models with highest Pearson correlation values are selected. The set of field data which measured from the laboratory tests are compared with the computed values which calculated from water indices, band ratios and combination bands of the satellite image for the study area.

The regression equations for each water quality parameter are revealed in Table (8) where the last equation for each parameter with the highest Pearson correlation values are selected to compute the value of the parameter.

The Figs. (9: 21) show the measured and computed value for each water quality parameter in the study area.

8	0.6918	0.7795	0.5276	0.6153	0.4507	0.5272	0.6212
9	0.3804	0.3629	0.2975	0.2799	0.1731	0.2737	0.1857
10	0.4608	0.4577	0.3588	0.3557	0.2281	0.3331	0.2581
11	0.4206	0.7432	0.3151	0.6377	0.5286	0.3115	0.5784
12	0.4445	0.7321	0.3358	0.6234	0.5086	0.3298	0.5684
13	0.6798	0.7343	0.5184	0.5729	0.4117	0.5186	0.5897
14	0.4199	0.4066	0.3270	0.3136	0.1969	0.3032	0.2195
15	0.4769	0.6223	0.3645	0.5099	0.3856	0.3527	0.4476
16	0.5055	0.7483	0.3823	0.6251	0.4997	0.3801	0.5940
17	0.4975	0.6737	0.3807	0.5570	0.4316	0.3722	0.5171
18	0.4672	0.7312	0.3543	0.6183	0.5002	0.3492	0.5738
19	0.4495	0.7296	0.3420	0.6220	0.5037	0.3312	0.5545
20	0.4740	0.7004	0.3583	0.5847	0.4647	0.3540	0.5390
21	0.4784	0.6425	0.3670	0.5311	0.4086	0.3559	0.4813
22	0.5374	0.6323	0.4087	0.5035	0.3690	0.4030	0.4737
23	0.3861	0.3744	0.3014	0.2897	0.1818	0.2782	0.1973
24	0.4154	0.4620	0.3225	0.3691	0.2565	0.3028	0.2892
25	0.3727	0.3871	0.2934	0.3078	0.2021	0.2669	0.2101
26	0.5522	0.7667	0.4189	0.6335	0.4917	0.4104	0.5805
27	0.7092	0.7973	0.5400	0.6282	0.4604	0.5414	0.6425
28	0.5979	0.7305	0.4532	0.5859	0.4358	0.4478	0.5484
29	0.6600	0.7422	0.5025	0.5847	0.4325	0.5078	0.6078
30	0.7211	0.7969	0.5443	0.6201	0.4537	0.5547	0.6584
31	0.4620	0.6283	0.3542	0.5204	0.4008	0.3424	0.4657
32	0.5108	0.6520	0.3912	0.5324	0.4038	0.3822	0.4950
33	0.5094	0.6044	0.3920	0.4870	0.3609	0.3833	0.4550
34	0.5093	0.6940	0.3881	0.5728	0.4398	0.3763	0.5078

Table (6): Band ratios used in the study area.

Sample	(C/B)	(C/G)	(C/R)	(C/NIR)	(NIR/(B+R))	(NIR/(B+NIR))	(B/(NIR+C))	(B/(R+C))
1	1.0819	1.0560	1.0157	0.5538	0.9460	0.6614	0.3294	0.4657
2	1.2318	1.6279	2.1702	2.1180	0.3710	0.3677	0.5515	0.5557
3	1.2089	1.5374	2.0287	3.1725	0.2388	0.2759	0.6289	0.5541
4	1.1137	1.1739	1.1112	0.5833	0.9536	0.6563	0.3308	0.4726
5	1.1290	1.2345	1.2830	0.5722	1.0496	0.6637	0.3224	0.4978
6	1.1931	1.4957	1.9444	2.3059	0.3207	0.3410	0.5846	0.5535
7	1.1972	1.4894	1.8999	2.5825	0.2844	0.3168	0.6021	0.5472
8	1.0831	1.0862	0.9657	0.6548	0.7796	0.6232	0.3653	0.4536
9	1.2232	1.5735	2.1713	3.0684	0.2550	0.2850	0.6166	0.5597
10	1.1874	1.4857	1.9038	1.9801	0.3693	0.3749	0.5596	0.5521
11	1.1991	1.2401	1.7418	0.3290	2.1586	0.7847	0.2064	0.5298
12	1.1768	1.2418	1.5696	0.3615	1.8608	0.7650	0.2256	0.5190
13	1.0564	1.0552	0.9113	0.7055	0.6935	0.5996	0.3916	0.4513
14	1.2021	1.5094	2.0051	2.4788	0.3032	0.3266	0.5928	0.5551
15	1.1696	1.2929	1.5311	0.6048	1.0964	0.6592	0.3222	0.5172
16	1.1393	1.1592	1.2535	0.4004	1.4905	0.7399	0.2510	0.4882
17	1.1437	1.2275	1.2795	0.4972	1.2145	0.6970	0.2904	0.4908
18	1.1671	1.2202	1.3998	0.3802	1.6741	0.7543	0.2360	0.4998
19	1.1847	1.3031	1.6798	0.3856	1.8015	0.7544	0.2349	0.5291
20	1.1648	1.2083	1.4199	0.4304	1.4868	0.7302	0.2583	0.5038
21	1.1562	1.2710	1.3755	0.5303	1.1845	0.6855	0.2997	0.5008
22	1.1093	1.1587	1.1929	0.6784	0.8472	0.6205	0.3644	0.4904
23	1.2169	1.5515	2.1113	2.6000	0.2969	0.3188	0.5935	0.5576
24	1.1995	1.4534	1.8048	1.1123	0.6478	0.5189	0.4390	0.5364
25	1.2241	1.6339	2.2218	1.7814	0.4430	0.4073	0.5232	0.5634
26	1.1336	1.2062	1.3815	0.4858	1.2818	0.7000	0.2884	0.5117
27	1.0703	1.0620	0.9328	0.6399	0.7789	0.6259	0.3646	0.4509
28	1.1169	1.1585	1.2365	0.6249	0.9390	0.6412	0.3443	0.4950
29	1.0924	1.0556	0.9033	0.6244	0.7918	0.6363	0.3519	0.4344
30	1.0513	0.9899	0.8626	0.6279	0.7546	0.6261	0.3669	0.4405
31	1.1605	1.2868	1.4487	0.5296	1.2167	0.6867	0.2983	0.5098
32	1.1315	1.2165	1.2428	0.5633	1.0515	0.6677	0.3184	0.4897
33	1.1475	1.2320	1.1926	0.6687	0.8745	0.6318	0.3492	0.4740
34	1.1595	1.2722	1.5277	0.5398	1.2213	0.6824	0.3023	0.5212

Table (7): The indices used in the study area.

Sample	NDWI	MNDWI	NDMI	WRI	NDVI	RVI	IPVI	DVI	AWEI
1	-0.31201	-0.1385	-0.29434	0.631768	0.294335	1.834206	0.647168	0.135573	-1.01142
2	0.130835	0.703053	-0.01216	1.855991	0.01216	1.02462	0.50608	0.001523	0.192267
3	0.347168	0.655518	0.219919	2.537732	-0.21992	0.639454	0.390041	-0.02423	0.203875
4	-0.33613	-0.09546	-0.31158	0.637893	0.311582	1.905213	0.655791	0.13069	-0.84395
5	-0.36661	-0.05393	-0.38318	0.599755	0.38318	2.242435	0.69159	0.153581	-0.69042
6	0.213119	0.722525	0.085049	2.184968	-0.08505	0.843235	0.457476	-0.01194	0.246486
7	0.268455	0.678373	0.152269	2.321726	-0.15227	0.735706	0.423866	-0.02029	0.226082
8	-0.24778	-0.17067	-0.19183	0.692038	0.191825	1.474712	0.595913	0.087664	-1.14341
9	0.322034	0.740254	0.17121	2.604974	-0.17121	0.707635	0.414395	-0.01758	0.220443
10	0.142642	0.665996	0.019653	1.872517	-0.01965	0.961452	0.490174	-0.00307	0.217879
11	-0.58065	0.01574	-0.68225	0.361303	0.682251	5.294275	0.841125	0.322594	-0.65178
12	-0.54911	0.097051	-0.62565	0.420584	0.625652	4.342619	0.812826	0.287564	-0.51541
13	-0.19862	-0.17419	-0.12729	0.739631	0.127288	1.291707	0.563644	0.054516	-1.07343
14	0.243073	0.695954	0.105645	2.223785	-0.10565	0.808899	0.447177	-0.01337	0.219794
15	-0.36259	0.194858	-0.43369	0.656013	0.433687	2.531619	0.716844	0.145383	-0.27091
16	-0.48649	-0.05479	-0.51577	0.479906	0.515771	3.130281	0.757886	0.242813	-0.80418
17	-0.42339	-0.02158	-0.44027	0.557794	0.440273	2.573171	0.720137	0.176247	-0.61924
18	-0.52488	0.010826	-0.57282	0.446912	0.572824	3.681911	0.786412	0.264001	-0.6694
19	-0.54329	0.062141	-0.62658	0.416638	0.626578	4.355878	0.813289	0.28006	-0.55952
20	-0.47473	-0.00663	-0.53481	0.484422	0.534815	3.299363	0.767407	0.226396	-0.63693
21	-0.41119	-0.0849	-0.44348	0.537097	0.443482	2.593777	0.721741	0.164063	-0.71278
22	-0.26142	-0.01886	-0.27494	0.717788	0.274935	1.758374	0.637468	0.094832	-0.57127
23	0.252569	0.611858	0.103736	2.071406	-0.10374	0.812027	0.448132	-0.01169	0.164768
24	-0.13292	0.346204	-0.23739	1.007262	0.237389	1.622568	0.618694	0.046587	-0.05271
25	0.043209	0.647415	-0.11001	1.534116	0.110009	1.247213	0.555004	0.014402	0.148485
26	-0.42579	0.129461	-0.47969	0.575671	0.479694	2.843888	0.739847	0.214547	-0.45352
27	-0.24803	-0.18445	-0.18626	0.687176	0.186258	1.457781	0.593129	0.088157	-1.2301
28	-0.29919	0.133059	-0.32853	0.739596	0.328525	1.978519	0.664263	0.132639	-0.39315
29	-0.25666	-0.15547	-0.18253	0.709006	0.182533	1.446581	0.591266	0.082199	-1.04133
30	-0.22374	-0.19311	-0.15743	0.702953	0.157435	1.373703	0.578717	0.075816	-1.24607
31	-0.41689	-0.00936	-0.46461	0.547513	0.464605	2.735562	0.732303	0.166258	-0.54135
32	-0.36704	-0.04481	-0.37625	0.608208	0.376253	2.206428	0.688126	0.14124	-0.67243
33	-0.29633	-0.04483	-0.28145	0.692418	0.281449	1.78338	0.640725	0.095011	-0.59743
34	-0.40424	0.156197	-0.47787	0.593726	0.477868	2.830448	0.738934	0.184736	-0.37516

Table (8): Models of the selected water quality parameters in the study area.

Parameter	Equation No.	Models (according to Eq. 7 and 8.)
pH	1	$pH = 8.278 + (-1.1 * DVI)$
EC	1	$EC = 269.526 + (361.393 * (C + NIR))$
	2	$EC = 39.913 + (880.169 * (C + NIR)) + (208.928 * MNDWI)$
	3	$EC = 1001.828 + (1264.679 * (C + NIR)) + (569.543 * MNDWI) + (-2297.831 * (B / (R + C)))$
	4	$EC = 1858.477 + (974.864 * (C + NIR)) + (886.688 * MNDWI) + (-3596.905 * (B / (R + C))) + (-140.787 * WRI)$
TH	1	$TH = 36.672 + (29.227 * (B + C + NIR))$
	2	$TH = 0.723 + (91.650 * (B + C + NIR)) + (26.492 * MNDWI)$
TDS	1	$TDS = 172.986 + (230.152 * (C + NIR))$
	2	$TDS = 26.338 + (561.481 * (C + NIR)) + (133.437 * MNDWI)$
	3	$TDS = 639.454 + (806.564 * (C + NIR)) + (363.290 * MNDWI) + (-1464.616 * (B / (R + C)))$
	4	$TDS = 1187.407 + (621.185 * (C + NIR)) + (566.151 * MNDWI) + (-2295.565 * (B / (R + C))) + (-90.054 * WRI)$
Turbidity	1	$Turbidity = 9.971 + (34.571 * DVI)$
Ca	1	$Ca = 21.675 + (18.761 * (B + C + NIR))$
	2	$Ca = -0.822 + (57.825 * (B + C + NIR)) + (16.578 * MNDWI)$
	3	$Ca = 35.535 + (67.353 * (B + C + NIR)) + (28.767 * MNDWI) + (-85.113 * (B / (R + C)))$
	4	$Ca = 117.593 + (41.627 * (B + C + NIR)) + (44.960 * MNDWI) + (-195.150 * (B / (R + C))) + (-41.461 * (B / (NIR + C)))$
K	1	$K = 5.322 + (0.356 * RVI)$
Na	1	$Na = 15.107 + (33.110 * ((C + B + G + NIR)))$
	2	$Na = -34.795 + (103.869 * ((C + B + G + NIR))) + (34.377 * MNDWI)$
Mg	1	$Mg = 8.586 + (6.537 * (C + NIR))$
	2	$Mg = 2.983 + (19.196 * (C + NIR)) + (5.098 * MNDWI)$
Cl	1	$Cl = 11.828 + (32.045 * (C + B + G + NIR))$

SO₄	2	$CI = -40.980 + (106.926 * (C+B+G+NIR)) + (36.380 * MNDWI)$
	1	$SO_4 = 9.013 + (33.072 * (C+B+G+NIR))$
	2	$SO_4 = -38.922 + (101.042 * (C+B+G+NIR)) + (33.022 * MNDWI)$
	3	$SO_4 = -0.304 + (-260.064 * (C+B+G+NIR)) + (64.026 * MNDWI) + (398.020 * (G+R+NIR))$
HCO₃	1	$HCO_3 = 124.885 + (86.750 * DVI)$
WQI	1	$WQI = 35.248 + (11.397 * (NIR/(B+R)))$

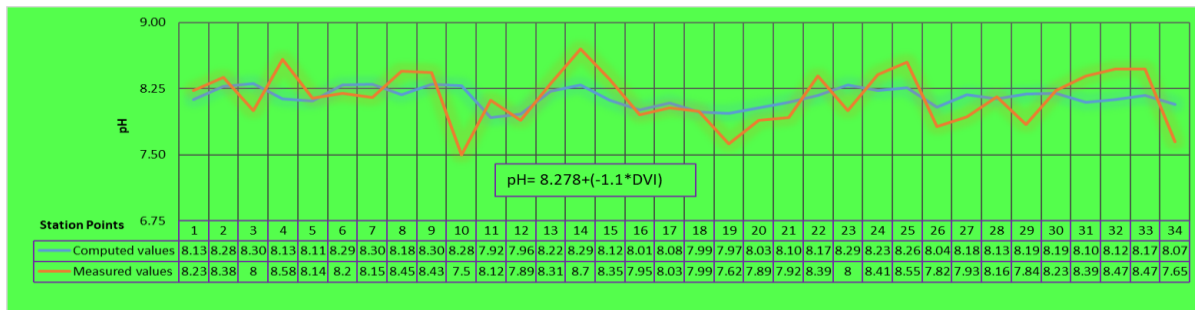


Fig. (9): Measured and computed pH values in the study area.

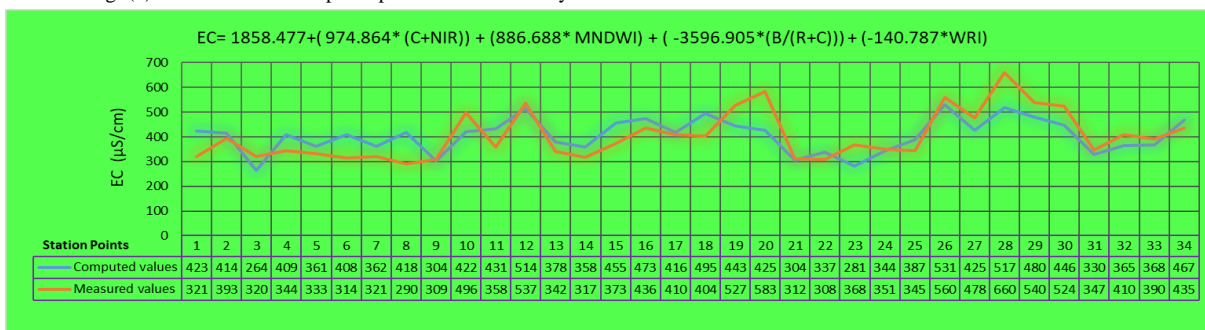


Fig. (10): Measured and computed EC values in the study area.

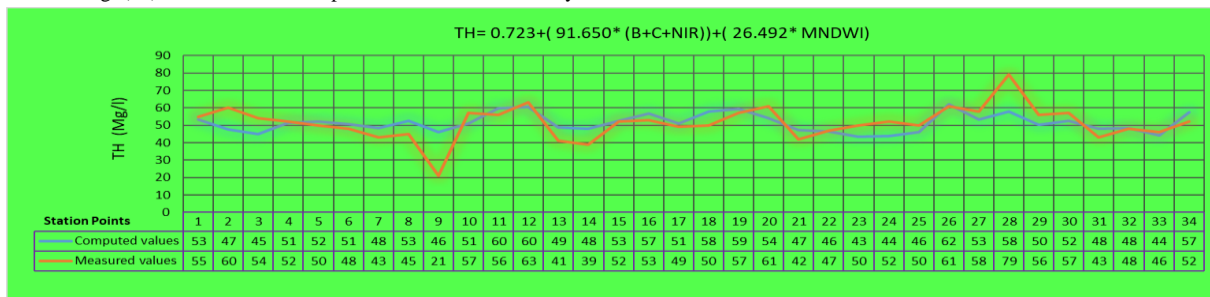


Fig. (11): Measured and computed TH values in the study area.

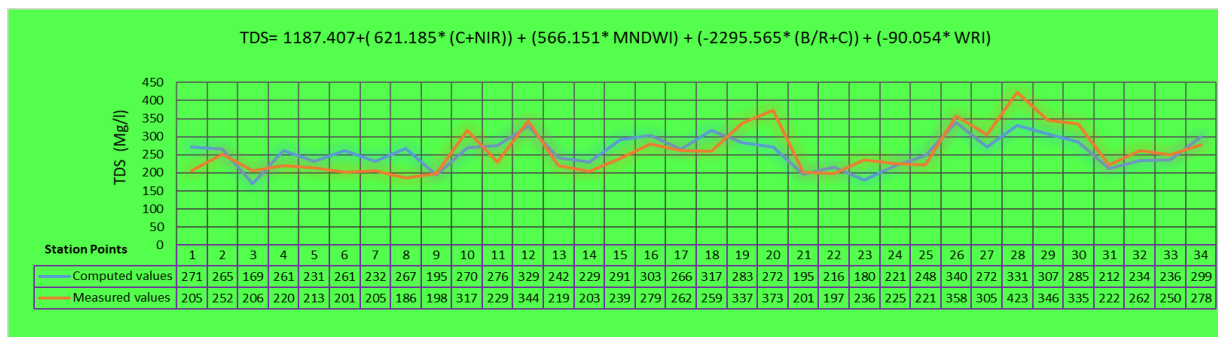


Fig. (12): Measured and computed TDS values in the study area.

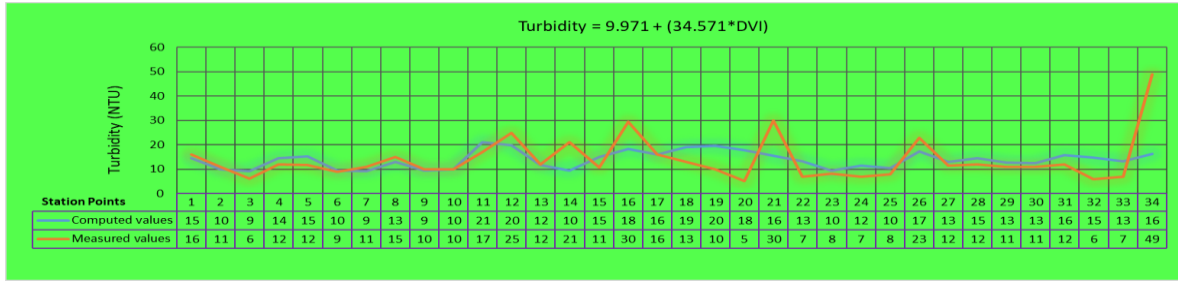


Fig. (13): Measured and computed turbidity values in the study area.

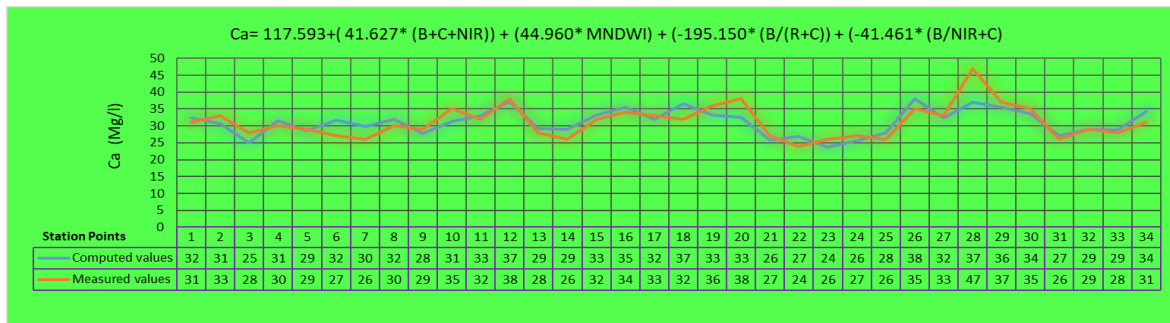


Fig. (14): Measured and computed Ca values in the study area.

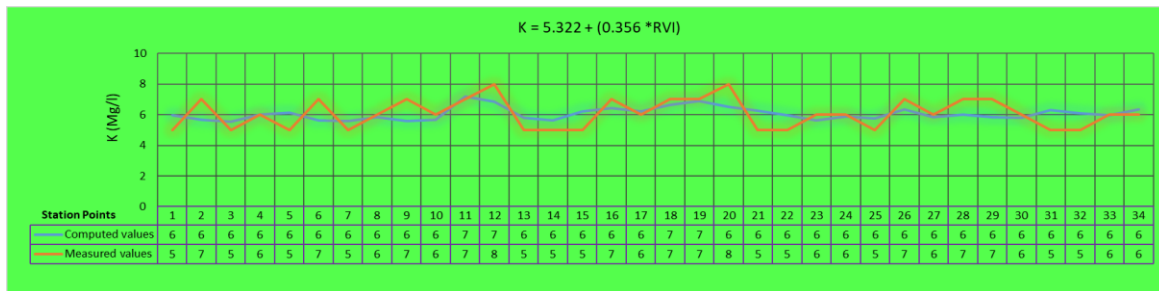


Fig. (15): Measured and computed K values in the study area.

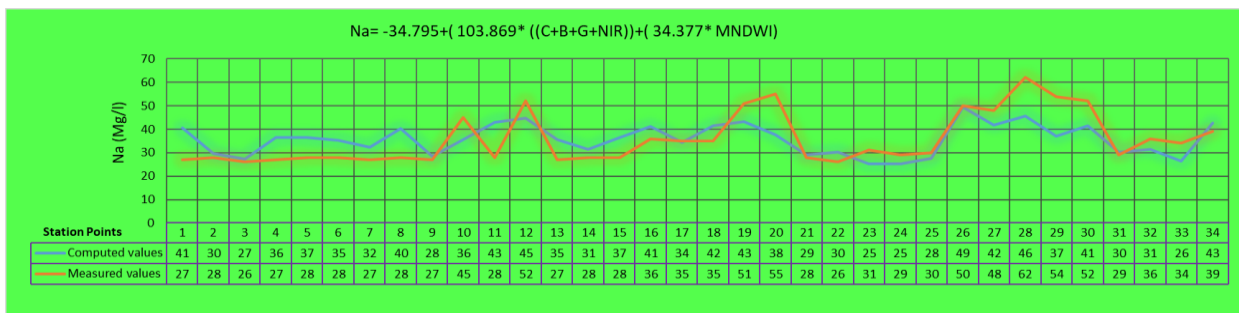


Fig. (16): Measured and computed Na values in the study area.

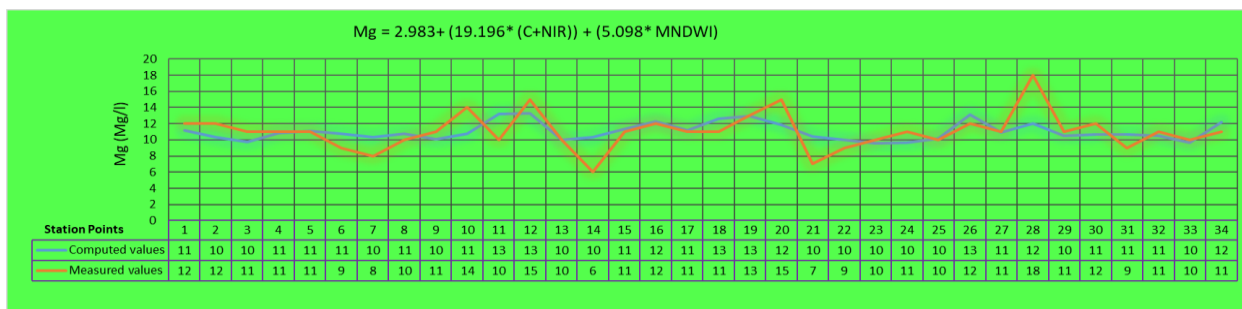


Fig. (17): Measured and computed Mg values in the study area.

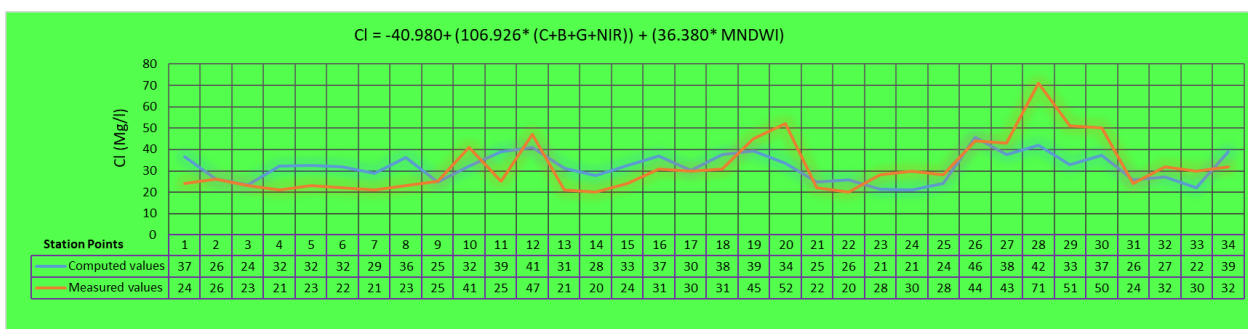


Fig. (18): Measured and computed Cl values in the study area.

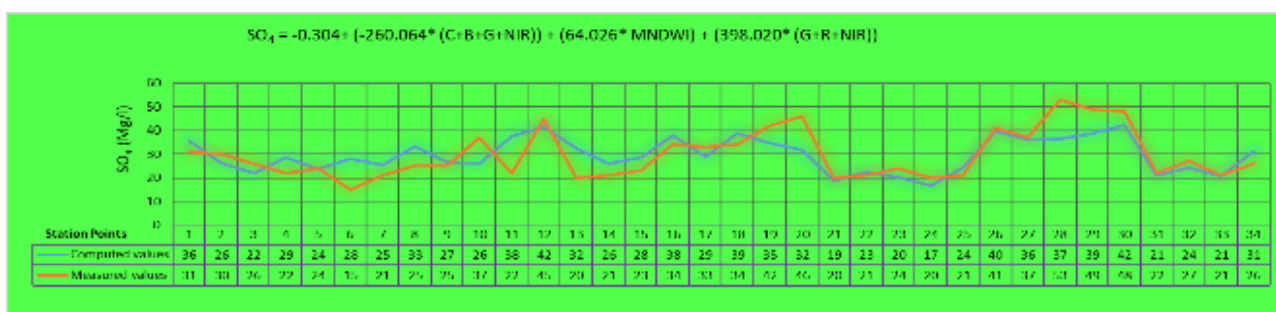


Fig. (19): Measured and computed SO₄ values in the study area.

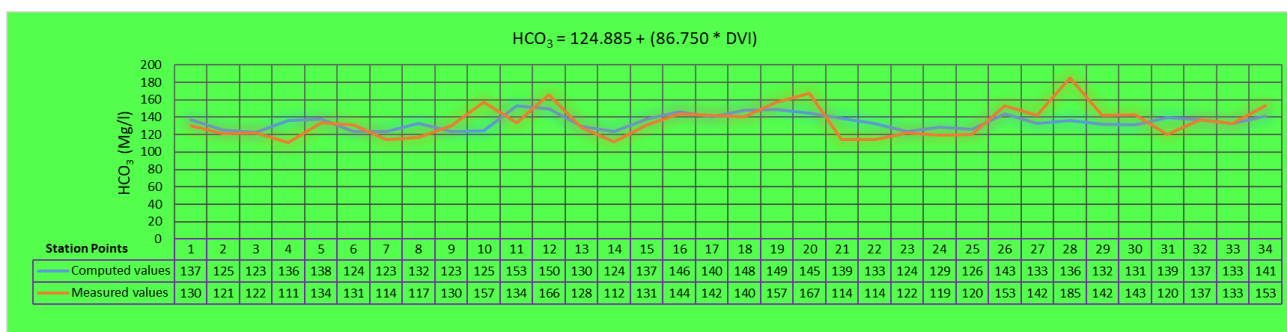


Fig. (20): Measured and computed HCO₃ values in the study area.

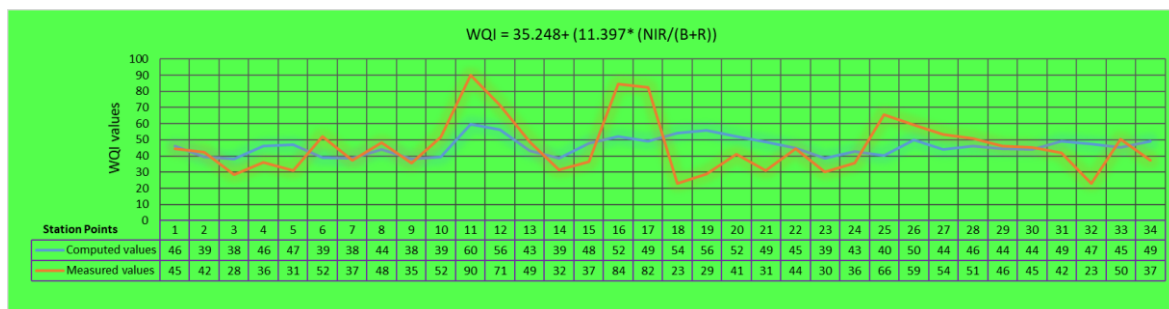


Fig. (21): Measured and computed WQI values in the study area.

5. Conclusions

In the present research, the water quality of the surface water in the study area was determined based on both the Landsat-8 (OLI) satellite data and the in-situ water quality measurements. There are four classes of WQI for surface water samples, about 6 % belong to the excellent class, 65% to good class, 20.6% to poor class and the rest of samples belong to very poor class, while no samples belong to unsuitable class. It could be noted that the very poor category of WQI belongs to Bahr Yusef Canal. Multispectral satellite images provide the whole information about the area under investigation. Many of digital processing techniques are used to extract most of the possible information from this image. Band transformation techniques generated new sets of image components which gives a good representation for land features, such as water, vegetations, bare lands and urban areas. The main classes obtained from the supervised classification show that the agricultural land dominated the whole study area with 75%, which might have an impact on water quality in the study area. The second dominant class is represented by urban areas with 11%. The third class was bare land with 10 %, which are distributed in several separate parts in the study area. The fourth class represented by water bodies with 4%. Spectral indices such as NDVI, NDBI, and NDWI are good for monitoring some land features in the study area. Finally, Landsat-8(OLI) images can be used to predict the water quality parameters and indices of surface water.

6. Acknowledgments

The author would like to thank Dr. Mahmoud Mostafa Khalil, Faculty of Science, Geology Department Minia University, Egypt.

7. References

1. Kairu, E.N., An introduction to remote sensing. *GeoJournal* 6, 251–260 (1982). <https://doi.org/10.1007/BF00210657>
2. Lwin, K.K., Fundamentals of remote sensing and its applications in GIS. Division of Spatial Information Science. University of Tsukuba. (2008). <http://giswin.geo.tsukuba.ac.jp/sis/tutorial/koko/remotesensing/FundamentalRemoteSensing.pdf>
3. Carlson, E. & Ecker, M. D., A Statistical Examination of Water Quality in Two Iowa Lakes. *American Journal of Undergraduate Research*, 1(2) (2002).
4. Dewidar, K., & Khedr, A. A., Remote sensing of water quality for Burullus Lake, Egypt. *Geocarto international*, 20(3), 43-49 (2005).
5. Fadhil, A. M., Environmental Change Monitoring by Geoinformation Technology for Baghdad and its Neighboring Areas, (2006). <http://www.GISdevelopment.net/Application/Environment.pdf>
6. Ming, S. Y., Carolyn, J. M. & Robert, M. S., Adaptive Short-Term Water Quality Forecasts Using Remote Sensing and Gis. *Awra Symposium on Gis And Water Resources*, Issue Sept 22-26 (1996).
7. Yas, N. M. S., A Study on Suspended Sediment Distribution in Himreen Reservoir Using Remote Sensing Techniques, M. Sc. Thesis, Building and Construction Engineering Department, University of Technology, Iraq, (2006).
8. Abdelmalik, K., Role of statistical remote sensing for Inland water quality parameters prediction, *The Egyptian Journal of Remote Sensing and Space Science*, 21, 193–200 (2018).
9. El-Zeiny, A. and El-Kafrawy, S., Assessment of water pollution induced by human activities in Burullus Lake using Landsat 8 operational land imager and GIS. *Egyptian Journal of Remote Sensing and Space Sciences*, 20: S49–S56 (2017).
10. APHA (American Public Health Association) Standard methods for examination of water and wastewater. 20th Ed. Washington, D C., P. 1193-2950 (2005).

11. Sanchez, E.; Colmenarejo, M. F.; Vicente, J.; Rubio, A.; Garcia, G.; Travieso, L. and Borja, R., Use of the Water Quality Index and dissolved oxygen deficit as simple indicators of watershed pollution, ecological indicators, *Ecol. Indic.*, 7 (1):315-328 (2007).
12. Hameed A, Alobaidy MJ, Abid HS, Mauloom BK., Application of water quality index for assessment of dokan lake ecosystem, Kurdistan region. *Iraq J Water ResourProt*, 2:792–798 (2010).
13. WHO (World Health Organization), Guidelines for Drinking-Water Quality, 4th ed.; WHO: Geneva, Switzerland, pp 155–202 (2011).
14. Yadav AK, Khan P, Sharma SK, Water quality index assessment of groundwater in Todaraisingh tehsil of Rajasthan state, India—a greener approach. *J Chem* 7: S428–S432 (2010).
15. Mårtensson, U., Introduction to remote sensing and geographical information systems. Remote sensing laboratory. Department of physical geography. University of Lund. Sweden (2011). https://www.nateko.lu.se/sites/nateko.lu.se.sv/files/remote_sensing_and_gis_20111212.pdf
16. Zanter, K., Landsat 8 (L8) data users handbook. Survey, Department of the Interior US Geological. (2015).
17. Nagelkerke, N. J., A note on a general definition of the coefficient of determination. *Biometrika*, 78(3), 691-692 (1991).
18. Steel, R. G., & James, H., Principles and procedures of statistics: with special reference to the biological sciences (No. 519.5 S314p). New York, US: McGraw-Hill (1960).
19. Liu, J. G., & Mason, P. J., Essential image processing and GIS for remote sensing. John Wiley & Sons (2013).
20. Mcfeeters, S.K., The use of normalized difference water index (NDWI) in the delineation of open water features, *International Journal of Remote Sensing*, 17, pp. 1425–1432 (1996).
21. Ko, B. C., Kim, H. H., & Nam, J. Y., Classification of potential water bodies using Landsat-8 OLI and a combination of two boosted random forest classifiers. *Sensors*, 15(6), 13763-13777 (2015).
22. Zhang, K., Thapa, B., Ross, M., & Gann, D., Remote sensing of seasonal changes and disturbances in mangrove forest: a case study from South Florida. *Ecosphere*, 7(6) (2016).
23. Feyisa, G. L., Meilby, H., Fensholt, R., & Proud, S. R., Automated Water Extraction Index: A new technique for surface water mapping using Landsat imagery. *Remote Sensing of Environment*, 140, 23-35 (2014).
24. Mukherjee, N. R., & Samuel, C., Assessment of the Temporal Variations of Surface Water Bodies in and around Chennai using Landsat Imagery. *Indian Journal of Science and Technology*, 9(18) (2016).
25. Richardson, A. J., & Wiegand, C. L., Distinguishing vegetation from soil background information. *Photogrammetric engineering and remote sensing*, 43(12), 1541-1552 (1977).
26. Ramachandra, T. V., Comparative assessment of techniques for bioresource monitoring using GIS and remote sensing. *The ICFAI Journal of Environmental Sciences*, 1(2) (2007)
27. Tucker, C. J., Red and photographic infrared linear combinations for monitoring vegetation. *Remote sensing of Environment*, 8(2), 127-150 (1979).
28. Gao, B. C., Normalized difference water index for remote sensing of vegetation liquid water from space. In *Imaging Spectrometry* (Vol. 2480, pp. 225-237). International Society for Optics and Photonics (1995).